



RAPID COMMUNICATION

Gene expression profiles contribute to robustly predicting prognosis in hepatocellular carcinoma



Hepatocellular carcinoma (HCC) is characterized by both inter- and intra-tumor heterogeneity and has distinct clinical outcomes.¹ A promising clinical tool to perform patient stratification, prognosis evaluation, and treatment recommendations is indispensable. Here, we enrolled a total of 1595 tumor patients from 13 independent cohorts, including seven cohorts with survival data, four cohorts with immunotherapy information, and two cohorts with transcatheter arterial chemoembolization (TACE) and Sorafenib information, respectively (Table S1). Using 96 algorithms combinations derived from 10 popular machine-learning approaches, a novel framework was constructed and described in Figure S1. Firstly, a total of 26 stable consensus prognostic genes were screened in seven cohorts harboring complete survival information via univariate Cox regression analysis (Fig. S2A). Then, these 26 genes were further subjected to our integrative machine learning-based framework to establish a consensus prognostic signature (CPIS). For a prognostic signature, superior generalization capability is a target leading research to be pursued, which means the signature still retains robust performance across different validation cohorts. Hence, the C-index was measured in the other six validation cohorts and the signature with the highest average C-index (0.682) was regarded as the optimal one, which was derived by the classical machine learning algorithm Ridge (Fig. 1A).

To further explore the clinical implications, patients were classified into high- and low-risk groups by the optimal cut-off value. The Kaplan–Meier survival analysis suggested that patients in the high-risk group presented conspicuous poor overall survival (OS) compared to the low-risk group in the TCGA-LIHC training cohort ($n = 363$, $P < 0.0001$), and similar results were produced in six validation cohorts as well as GSE14520 ($n = 242$, $P < 0.0001$), GSE54236 ($n = 81$,

$P < 0.0001$), GSE116174 ($n = 64$, $P = 0.0014$), GSE144269 ($n = 68$, $P = 0.0131$), E-TABM-36 ($n = 39$, $P = 0.0037$), ICGC-LIRI ($n = 232$, $P < 0.0001$), and Meta-Cohort ($n = 1089$, $P < 0.0001$) (Fig. 1B–I). In addition, TCGA-LIHC and GSE14520 with complete recurrence-free survival (RFS) were also exploited to elucidate prognostic significance. Likewise, patients in the high-risk group had a superior relapse rate relative to those in the low-risk group (TCGA-LIHC, $n = 313$, $P < 0.0001$; GSE14520, $n = 242$, $P = 0.0002$) (Fig. 1J, K).

The time-dependent area under the ROC curves (AUCs) of CPIS almost exceeded 0.7 at 1/2/3 years, which demonstrated the favorable discriminative ability (Fig. S2B). The calibration curves of CPIS also elucidated its performance at accurately predicting prognosis across eight cohorts (Fig. S2C–J). The detailed AUCs of all cohorts were as follows: TCGA-LIHC (0.762/0.737/0.717), GSE14520 (0.650/0.668/0.670), GSE54236 (0.801/0.705/0.738), GSE116174 (0.781/0.724/0.693), GSE144269 (0.707/0.662/0.651), E-TABM-36 (0.757/0.763/0.771), ICGC-LIRI (0.793/0.793/0.817), and Meta-Cohort (0.741/0.712/0.689) (Fig. S3A–H). Overall, the above results shed light on CPIS generated from 96 algorithm combinations, which could robustly predict the prognosis of HCC patients.

In addition, certain clinicopathological traits (such as BCLC stage, TNM stage, and grade) and molecular features (such as *CTNNB1* mutation) are usually applied to the prognostic evaluation and clinical management.^{2,3} An interesting idea is to compare the CPIS with other clinical and molecular variables to assess the performance of predicting prognosis. Notably, our CPIS displayed distinctly superior accuracy than routine clinical traits encompassing age, gender, BMI, HBV, HCV, HDV, TNM stage, grade, cirrhosis, and *CTNNB1* mutation, apart from the comparison between CPIS and TNM stage in GSE14520 (Fig. S3I–O). In these cohorts, the C-index [95% confidence interval] was 0.688 [0.663–0.714], 0.630 [0.600–0.660], 0.667

Peer review under responsibility of Chongqing Medical University.

<https://doi.org/10.1016/j.gendis.2023.01.025>

2352-3042/© 2023 The Authors. Publishing services by Elsevier B.V. on behalf of KeAi Communications Co., Ltd. This is an open access article under the CC BY-NC-ND license (<http://creativecommons.org/licenses/by-nc-nd/4.0/>).

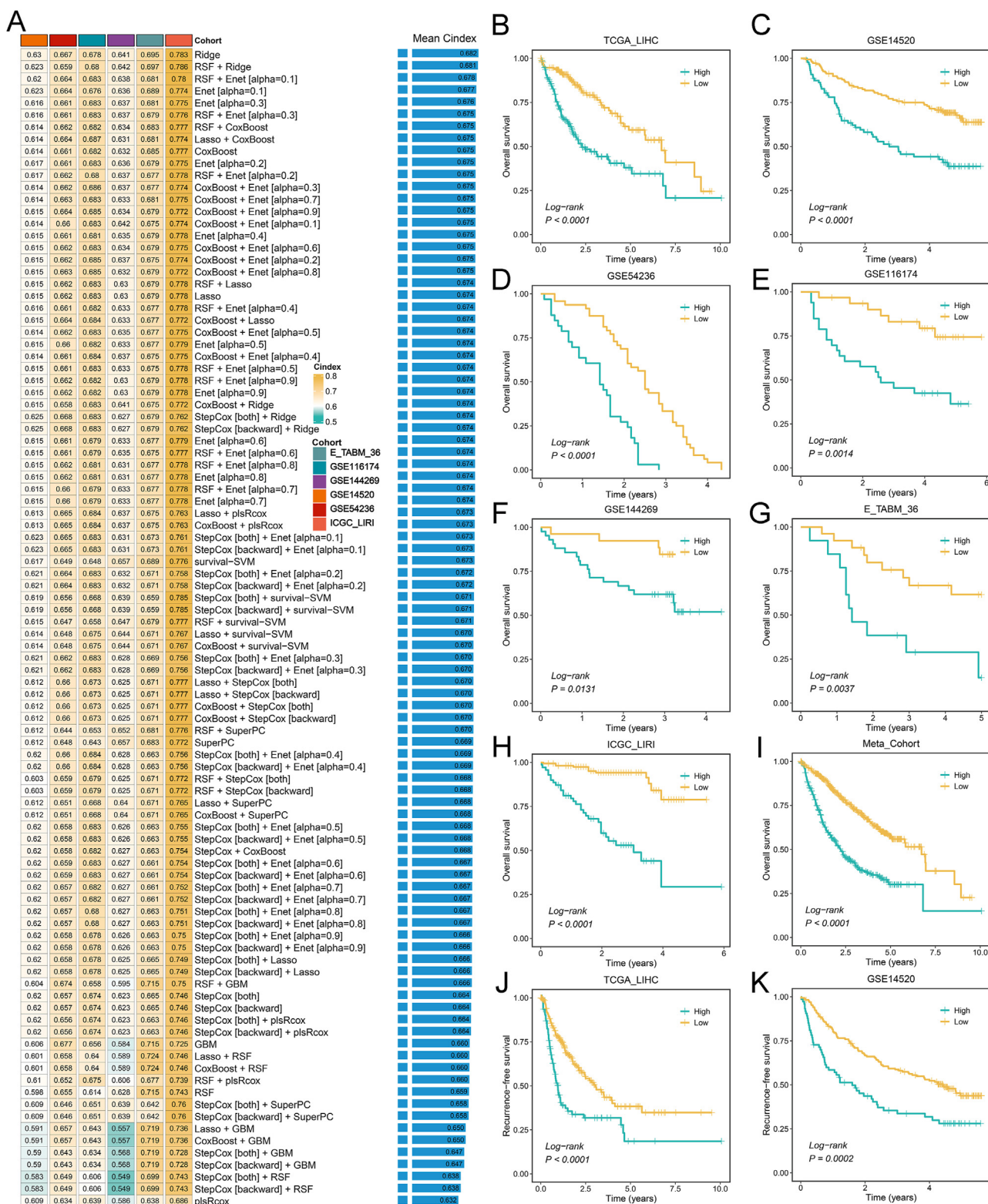


Figure 1 A consensus prognostic signature was developed and validated via the integrative machine learning algorithm. (A) The C-indexes of 96 kinds of prediction models across seven validation cohorts. (B–I) Kaplan–Meier curves of OS according to the CPIS in (B) TCGA-LIHC ($n = 363$, $P < 0.0001$), (C) GSE14520 ($n = 242$, $P < 0.0001$), (D) GSE54236 ($n = 81$, $P < 0.0001$), (E) GSE116174 ($n = 64$, $P = 0.0014$), (F) GSE144269 ($n = 68$, $P = 0.0131$), (G) E-TABM-36 ($n = 39$, $P = 0.0037$), (H) ICGC-LIRI ($n = 232$, $P < 0.0001$), and (I) Meta-Cohort ($n = 1089$, $P < 0.0001$). (J, K) Kaplan–Meier curves of RFS according to the CPIS in (J) TCGA-LIHC ($n = 313$, $P < 0.0001$) and (K) GSE14520 ($n = 242$, $P = 0.0002$).

[0.632–0.703], 0.678 [0.628–0.728], 0.641 [0.582–0.700], 0.695 [0.642–0.748], 0.783 [0.747–0.819], and 0.669 [0.655–0.683], respectively (Fig. S3P). Multivariate Cox regression also suggested that CPIS performed statistically significant ($P < 0.05$) for OS when adjusted for available clinical and molecular traits, which indicated CPIS could be regarded as an independent prognostic indicator for HCC (Table S2). Therefore, our CPIS could be a promising tool for prognostic evaluation and patient stratification in clinical practice, further improving clinical management.

Currently, with advancements in sequencing techniques and artificial intelligence, conspicuously increasing predictive gene expression signatures have been put forward based on diverse machine learning algorithms.⁴ To compare the performance of CPIS with previously published signatures, we comprehensively enrolled 100 prognostic signatures, including lncRNA and mRNA signatures while miRNA signatures were excluded due to the lack of miRNA expression information (Table S3). Impressively, Cox regression analysis suggested only our CPIS exhibited consistent significance in all datasets, proving its stability (Fig. S4A). We further calculated the C-index of CPIS and compared it with other published signatures. As illustrated in Figure S4B, the CPIS presented a better performance in most cohorts and ranked first or forefront, except for the TCGA-LIHC cohort. We noticed that signatures performed well and ranked first or second in TCGA-LIHC but performed weakly in external datasets and even closed to the bottom in GSE116174 (e.g., Zhou-FCDB), GSE144269 (e.g., Zhou-BR). This may be explained owing to the poor generalization ability caused by overfitting. All the results suggested our CPIS boasted excellent robustness and possessed better extrapolation potential.

Various molecular characteristics could map into distinct clinical outcomes. Thus, we further decoded the landscape of genomic variations and explored underlying biological mechanisms for patients. Notably, patients with high CPIS harbored dramatically superior CNA relative to patients with low CPIS, such as amplification of 10p15.1 and deletion of 4q21.3, 4q24, and 16q23.1 (Fig. S5A). Thus, patients with high CPIS conveyed prominent genomic variations, hinting at high genomic instability. Using the *limma* package, we identified differentially expressed genes between two groups (Fig. S6A). Based on gene sets from Hallmark, the top 10 observably enriched pathways were displayed according to normalized enrichment score (NES) respectively. Intriguingly, patients with high CPIS enriched numerous pathways associated with cell cycle and proliferation, such as E2F targets and G2M checkpoint, while patients with low CPIS presented dominantly related to biological metabolisms, such as fatty acid metabolism and fatty acid metabolism (Fig. S5B). Moreover, popular treatments in clinical practice were also used to assess the predictive value of CPIS for quantifying therapeutic benefits. Our results suggested that patients with low CPIS were recommended to take more consideration for TACE and Sorafenib (Fig. S6B, C). Overall, all these characteristics of genomic variations and biological functions might provide new insights into feasible therapeutic targets for improving clinical outcomes.

Accumulating evidence has revealed tumor microenvironment (TME) is implicated in immunotherapy responses

and clinical outcomes.⁵ To yield more detailed insights into TME characteristics, the 28 immune cell infiltrations were further estimated. Most immune cells displayed more elevated infiltration in the low-risk group, such as activated CD8 T cells and natural killer cells (Fig. S5C, 7A). Correlation analysis also highlighted most immune cells were significantly inverse links with CPIS (Fig. S7B). Collectively, patients with low CPIS presented a superior immune infiltration, indicating more backup resources for immunotherapy. Moreover, we extended our exploration to HLA molecules, co-stimulatory molecules, and co-inhibitory molecules. The results elucidated that patients in the low-risk group possessed higher expression of most molecules, such as *HLA-DPA1*, *CD226*, and *CD274*, while the expression of some molecules was elevated in the high-risk group, such as *CD58* and *TNFSF4* (Fig. S7C, 7D, 6D). These discoveries might bring foundations for clinical management, facilitating immunotherapy efficacy. Therefore, four cohorts with immunotherapy, including 57 responders and 149 non-responders, were enrolled to further evaluate the performance of CPIS at quantifying clinical benefits. There was a conspicuous tendency that patients in the low-risk group presented a high fraction of response in GSE35640, GSE100797, GSE91061, and Nathanson cohorts (Fig. S7E–H). Taken together, patients with low CPIS tended to be sensitive to immunotherapy and CPIS might be a favorable tool for immunotherapy estimation.

In conclusion, to improve clinical outcomes and guide an individualized approach, our study developed a robust and promising consensus prognostic signature for patient stratification, prognosis evaluation, and treatment recommendations according to bioinformatics and machine learning algorithms.

Author contributions

Long Liu and Zaoqu Liu contributed to study design, data analysis, and paper writing. Xinwei Han contributed to project oversight and paper revisiting. Yuhui Wang and Yuyuan Zhang contributed to the paper writing and revising. Yuhui Wang, Siyuan Weng, and Hui Xu collected samples and generated data. All authors read and agreed to publish the final version of the manuscript.

Conflict of interests

The authors declare that they have no competing interests.

Funding

This work was supported by the Henan Province Medical Research Project, Henan, China (No. LHGJ20190388).

Appendix A. Supplementary data

Supplementary data to this article can be found online at <https://doi.org/10.1016/j.gendis.2023.01.025>.

References

1. Yang C, Zhang H, Zhang L, et al. Evolving therapeutic landscape of advanced hepatocellular carcinoma. *Nat Rev Gastroenterol Hepatol.* 2023;20(4):203–222.
 2. Reig M, Forner A, Rimola J, et al. BCLC strategy for prognosis prediction and treatment recommendation: The 2022 update. *J Hepatol.* 2022;76(3):681–693.
 3. Chen LJ, Chang YJ, Chang YJ. Survival predictability between the American joint committee on cancer 8th edition staging system and the Barcelona clinic liver cancer classification in patients with hepatocellular carcinoma. *Oncol.* 2021;26(3):e445–e453.
 4. Piñero F, Dirchwolf M, Pessôa MG. Biomarkers in hepatocellular carcinoma: diagnosis, prognosis and treatment response assessment. *Cells.* 2020;9(6):1370.
 5. Liu Z, Zhang Y, Shi C, et al. A novel immune classification reveals distinct immune escape mechanism and genomic alterations: implications for immunotherapy in hepatocellular carcinoma. *J Transl Med.* 2021;19(1):5.
- Long Liu^{a,1}, Yuhui Wang^{b,1}, Yuyuan Zhang^c, Siyuan Weng^c, Hui Xu^c, Zaoqu Liu^{c,d,e,**}, Xinwei Han^{c,d,e,*}
- ^aDepartment of Hepatobiliary and Pancreatic Surgery, The First Affiliated Hospital of Zhengzhou University, Zhengzhou, Henan 450052, China
- ^bPrenatal Diagnosis Center, The Third Affiliated Hospital of Zhengzhou University, Zhengzhou, Henan 450052, China
- ^cDepartment of Interventional Radiology, The First Affiliated Hospital of Zhengzhou University, Zhengzhou, Henan 450052, China
- ^dInterventional Institute of Zhengzhou University, Zhengzhou, Henan 450052, China
- ^eInterventional Treatment and Clinical Research Center of Henan Province, Zhengzhou, Henan 450052, China
- *Corresponding author. Department of Interventional Radiology, The First Affiliated Hospital of Zhengzhou University, Zhengzhou, Henan 450052, China.
- **Corresponding author. Department of Interventional Radiology, The First Affiliated Hospital of Zhengzhou University, Zhengzhou, Henan 450052, China.
E-mail addresses: liuzaoqu@163.com (Z. Liu), fcchanxw@zzu.edu.cn (X. Han)

13 November 2022
Available online 24 March 2023

¹ These authors contributed equally to this work and shared the first authorship.